



Highly specific colorimetric detection of DNA oxidation biomarker using gold nanoparticle/triplex DNA conjugates

Xun Gao, PhD^{a,1}, Yung-Hao Tsou, PhD^{b,1}, Marina Garis^b,
Haidong Huang, PhD^{a,*}, Xiaoyang Xu, PhD^{b,*}

^aDepartment of Chemistry and Environmental Science, New Jersey Institute of Technology, Newark, NJ, USA

^bDepartment of Chemical, Biological, and Pharmaceutical Engineering, New Jersey Institute of Technology, Newark, NJ, USA

Received 11 January 2016; accepted 18 May 2016

Abstract

DNA oxidation causes a variety of diseases including cancer. The oxidized DNA nucleobases are excised by cellular repair enzymes and released into extracellular fluids. Specifically, the excised DNA oxidation product, such as 8-oxoGua, has been suggested as a biomarker for early cancer diagnosis. We previously developed an artificial receptor for the free base of 8-oxoGua on a triplex DNA backbone. The receptor contained a pre-organized cavity, which bounded 8-oxoGua with strong affinity and excellent selectivity over other nucleobases. However, accurate detection of 8-oxoGua in urine samples was affected by the presence of a large excess of guanine. Herein, we report a strategy to convert our receptor to a colorimetric biosensor by conjugating DNA strands to gold nanoparticles (GNP), specifically for 8-oxoGua. By simply incubating our sensor with a urine sample, 8-oxoGua can be detected at submicromolar concentrations with UV–vis spectrometer or even by naked eye.

© 2016 Published by Elsevier Inc.

Key words: Nanoparticle; DNA oxidation; Colorimetric detection; Oligonucleotide

Triplex DNA containing single-nucleotide gaps has been used as the molecular skeleton to design synthetic receptors for small nucleobase and nucleoside targets.^{1–5} Strong and highly selective binding has been achieved by engineering the cavity to create complementary binding surfaces. The targets are sandwiched by the flanking nucleobases through π – π stacking interactions, and simultaneously by the pairing bases through Watson–Crick and Hoogsteen hydrogen bonding interactions. The DNA sandwich systems can be used as artificial sensors for the detection of biologically important small molecules such as excised DNA oxidation product 8-oxo-7, 8-dihydroguanine (8-oxoGua). 8-OxoGua is an oxidized form of guanine where its source in extracellular fluid comes from the enzymatic repair of 8-oxo-7, 8-dihydro-2'-deoxyguanosine (8-oxodG) in DNA. As such, 8-oxoGua was viewed as a urinary DNA oxidative damage biomarker for early cancer stage diagnosis.⁶ The current 8-oxoGua detection methods include gas chromatography/liquid

chromatography–mass spectrometry (GC/LC–MS), LC–electrochemical detection, and competitive enzyme-linked immunosorbent assays (ELISA).^{7–10}

A triplex DNA receptor approach for 8-oxoGua detection has also been developed.² Pyrrolo-C, a fluorescent cytosine analogue, was incorporated to the receptor as the signal reporter. Addition of 8-oxoGua caused remarkable fluorescence quenching in which the change of fluorescent intensity can be monitored by a fluorimeter. The detection range of the sensors was 3 nM–1 μ M, comparable with the commercial immunoassay kit from Trevigen, which non-selectively detects 8-oxoGua and its 2'-deoxyribonucleosides and ribonucleosides.^{7,8} While the ELISA kits cross-react with urea in urine samples¹¹ detection with fluorescence sensors is less affected. However, the fluorescence sensors overestimate 8-oxoGua concentrations by 1.5–2.0 folds as a result of the interference from urinary guanine, whereas urine typically contains 13 times higher concentration of guanine than 8-oxoGua.² Additionally, fluorescent dyes in general suffer from photobleaching. Hence, a more reliable method that completely distinguishes 8-oxoGua from guanine is highly desirable. Herein we report a simple, fast and low-cost colorimetric method to measure 8-oxoGua concentration using DNA modified gold nanoparticle as sensing probes, which

*Corresponding authors.

E-mail addresses: haidong.huang@njit.edu (H. Huang),
xiaoyang@njit.edu (X. Xu).

¹ Authors contribute equally.

<http://dx.doi.org/10.1016/j.nano.2016.05.011>

1549-9634/© 2016 Published by Elsevier Inc.

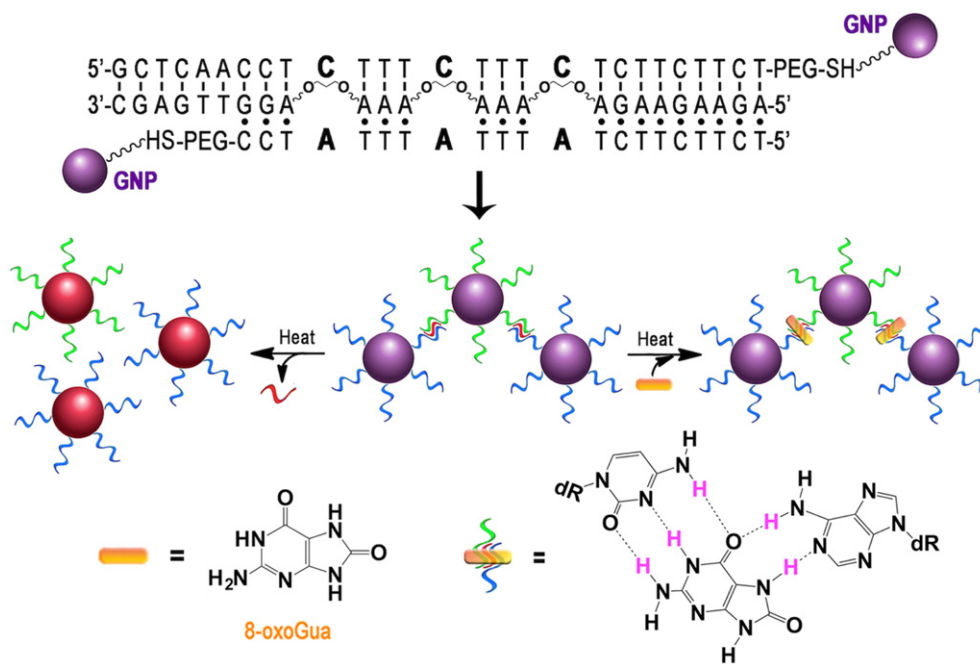


Figure 1. Schematic illustration of DNA-GNP based colorimetric sensor for 8-oxoGua detection.

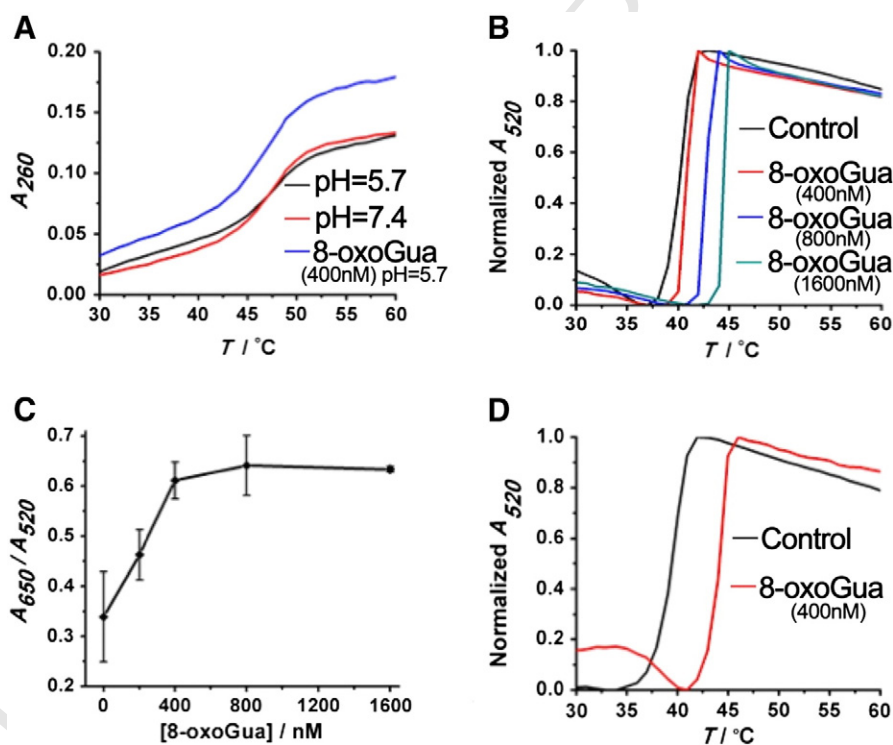


Figure 2. (A) Melting curves of GNP-free triplex or duplex DNA monitored at 260 nm. (B) Melting curves of GNP aggregates in the presence of different concentrations of 8-oxoGua. (C) Plot of absorption ratio (A_{650}/A_{520}) vs. different concentrations of 8-oxoGua at 41 °C. (D) Melting curves of GNP aggregates at a lower GNP concentration. (More details in supporting materials.)

enables the detection of 8-oxoGua by UV-vis spectrometer or even naked eye in a high-throughput fashion.

DNA modified Au nanoparticles have been widely used for assembly,^{1,12,13} sensing,^{1,14-17} bio-imaging,^{1,18} and drug

delivery.^{1,19,20} Conjugation of nucleic acids to Au nanoparticle allows convenient modification of the nanoparticle surfaces and precise control of the particle aggregation through DNA hybridization. DNA Au NPs have high extinction coefficients

t1.1 Table 1

t1.2 Melting temperatures in different conditions [a].

t1.3 Entry	[GNP-DNA] (nM)	[8-oxoGua] (nM)	T_m (°C) ^[b]
t1.4 1	2	0	40.0
t1.5 2	2	400	42.0
t1.6 3	2	800	43.9
t1.7 4	2	1600	46.0
t1.8 5	1	0	40.1
t1.9 6	1	400	44.0
t1.10 7 ^[c]	1	0	41.0
t1.11 8 ^[c]	1	400	43.0

[a] Buffer conditions: PBS, 10 mM, PIPES, 100 mM, additional NaCl, 100 mM, MgCl₂, 10 mM, SDS, 0.1% wt, pH 5.7. [b] Average of the three measurements. [c] Urine mimic was added 2 h after the hybridization.

t1.12

(about four orders of magnitude greater than typical organic dyes), sharp melting transition and unique distance-dependent plasmonic properties.²¹ These unique properties allow us to build a GNP-linked triplex receptor (Figure 1) to selectively detect 8-oxoGua in the presence of guanine. The two pyrimidine-rich strands of the receptor were conjugated to GNPs via 3'-thiol modification. These two strands are non-complementary and thus do not interact with each other. The purine-rich strand, which contained three C3 spacers, functioned as a linker to induce GNP aggregation. The purpose of using three C3 spacers was to amplify the stabilization effect caused by the binding of 8-oxoGua. The same triplex DNA in the absence of GNPs does not show clear triplex-to-duplex transition in a UV melting experiment above 20 °C (Figure 2, A), indicating the three C3 spacers separated by two -AAA- regions greatly destabilize the triplex formation. It is noteworthy to mention that binding of guanine to the cavities is likely to occur without the participation of the parallel pyrimidine-rich region. Therefore, urinary guanine was not expected to affect the melting of aggregated GNPs and the resulting purple-to-red color change.

We first examined the relationship between the concentrations of 8-oxoGua or guanine and the thermal stability of the triple helix. The thermal stability was determined through a series of UV-vis melting experiments monitored at wavelength of 520 nm. The samples of the experiments were prepared by hybridizing the two GNP-DNA conjugates (2 nM each) and the linker in the presence of 8-oxoGua. A sharp melting transition was observed in each experiment (Figure 2, B), indicating a cooperative dissociation of GNP aggregates (Figure S1) and formation of well-suspended red nanoparticles. The stabilization effect was concentration-dependent. Within the 8-oxoGua concentration range of 400 nM–1600 nM, each doubling of the concentration increased the melting temperature by approximately 2 °C (Table 1). These sharp melting transitions allow relatively wide temperature windows to distinguish two samples with different 8-oxoGua concentrations.

After the temperature windows for detection were established, we then carried out the in situ colorimetric assays. The goal of the colorimetric assays was to detect target molecules in biological samples conveniently, economically, and rapidly. When the same GNP aggregates were incubated with 8-oxoGua, adenine, guanine, cytosine, and thymine (400 nM each) at 40 °C for 2 min, only the sample containing 8-oxoGua remained pink (Figure 3, A), whereas

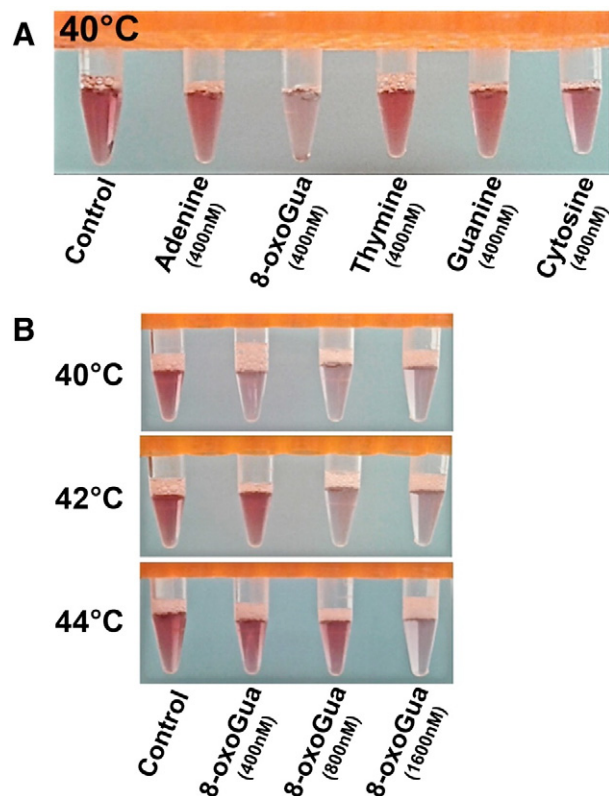


Figure 3. Colorimetric assays of GNP-DNA aggregates after incubation (A) under 40 °C for 2 minutes in presence of different nucleobases (B) under different temperatures in presence of different concentrations of 8-oxoGua. (More details in supporting materials.)

the control sample turned red. This observation was consistent with the visible spectrum of the GNP suspension, which showed significant blue shift when 8-oxoGua was added. (Figure S2). Notably, the samples in the presence of other potential interfering species also turned red. This experiment demonstrated that our assay could effectively discriminate between 8-oxoGua and other nucleobases. The same assay was used to qualitatively examine the concentration of 8-oxoGua (Figure 3, B). As expected, the 8-oxoGua-free sample melted and turned red at 40 °C, while the other samples containing 8-oxoGua (400–1600 nM) remained pink. At 42 °C, the sample containing 400 nM 8-oxoGua turned red. At 44 °C, the sample containing 800 nM 8-oxoGua also turned red. The only sample that remained pink was in the presence of 1600 nM 8-oxoGua. These colorimetric performances of the GNP aggregates under mild heating were consistent with the above UV-vis melting results. The sensor may be used for a wide range of different applications since the threshold of detection was temperature-dependent.

The ratio of absorbance at two wavelengths (A_{650}/A_{520}) recorded on a UV-vis spectrometer was plotted against 8-oxoGua concentrations to generate an 8-oxoGua response curve. This curve may be used to quantitatively determine the concentration of 8-oxoGua in an unknown sample (Figure 2, C). The limit of detection using the spectrometer was determined to be 128 nM. Although the detection limit was higher than that of our previous fluorescent sensor, the response range still covers a major portion of the biologically relevant concentration range.

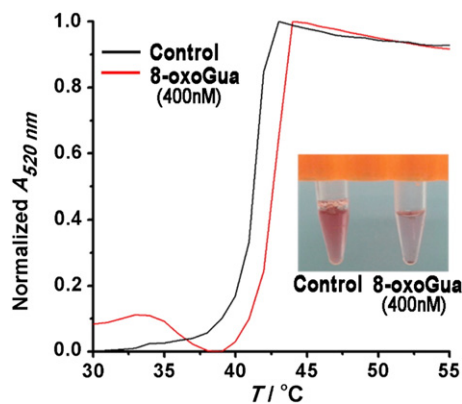


Figure 4. Melting curves of GNP-DNA aggregates in urine mimic. (More details in supporting materials.)

We then examined the possibility of further promoting the sensitivity by lowering the amount of GNP aggregates in the assay. Binding of 8-oxoGua to the three consecutive cavities of each triplex was very likely to be positively cooperative due to the effect of binding-induced preorganization. 200 nM of 8-oxoGua would only be able to bind one of the three cavities in each receptor with a weak binding constant. By lowering the GNP concentration from 2 nM to 1 nM, the same amount of 8-oxoGua was expected to occupy a larger portion of the cavities with a stronger binding constant, thereby generating a more dramatic helical stabilization effect. Certainly, the melting temperature difference was 4 °C when 400 nM 8-oxoGua was added to 1 nM GNP aggregates (Figure 2, D, Table 1), compared to 2 °C when the same amount of 8-oxoGua was added to 2 nM GNP aggregates.

To demonstrate that our colorimetric assays can be used practically for urinary detection of 8-oxoGua, and in particular to overcome the influence of the coexisting highly concentrated nucleobases, we performed the melting study and the colorimetric assay in the presence of a urine mimic containing 100 mM urea, 4 μM adenine, 0.4 μM cytosine, 1.2 μM guanine, and 6 μM uracil.²² The urine mimic sample with and without 400 nM 8-oxoGua was incubated with GNP aggregates (1 nM) at room temperature for 2 h. Melting experiment results showed that the unspiked sample melted at 41 °C (Figure 4, A), which was slightly higher than the melting temperature in the absence of the urine mimic (40 °C). This difference is likely to be caused by non-specific binding of nucleobases in urine. The melting temperature of the spiked sample increased to 43 °C, suggesting that 8-oxoGua can compete with the non-specific binding and induce a larger stabilization effect. The colorimetric assay showed a clear red versus pink difference when comparing the unspiked and spiked samples, which is consistent with the results of the melting experiments (Figure 4, B).

Although many methods have been reported to quantify 8-oxoGua concentrations in urine, the absolute amount of 8-oxoGua in concentration units or nmol/24 h has been reported on only limited occasions. The reported average 8-oxoGua concentrations ranged from 90 to 580 nM.^{9,10,23} A major advantage of our sensor, in addition to its specificity, is the detection range in which it can be tuned by using different GNP

concentrations and incubation temperatures. Therefore, a 177 protocol for each specific application can be generated to meet 178 the clinical demand for 8-oxoGua quantification. 179

In summary, assembling of multi-gapped triplex receptors 180 was facilitated by conjugation of the two pyrimidine-rich DNA 181 strands to gold nanoparticles. Target molecules such as 182 8-oxoGua can enter the triplex cavities and stabilize the pink 183 aggregates. The presence of multiple binding cavities has 184 enhanced the binding-induced stabilization effect and widened 185 the temperature window used for detection. The triplex-specific 186 melting process enhanced the detection selectivity for 8-oxoGua 187 over guanine, a commonly known interfering species. For the 188 first time, 8-oxoGua can be directly detected at sub-micromolar 189 concentrations without using a major instrument. This methodology 190 may become a universal solution to the detection of nucleobases and 191 nucleosides in biological fluids. 192

Appendix A. Supplementary data

Supplementary data to this article can be found online at 194 <http://dx.doi.org/10.1016/j.nano.2016.05.011>. 195

References

- Patel M, Dutta A, Huang H. A selective adenosine sensor derived from a 198 triplex DNA aptamer. *Anal Bioanal Chem* 2011;**400**:3035–40. 199
- Zhang Q, Wang Y, Meng X, Dhar R, Huang H. Triple-stranded DNA 200 containing 8-oxo-7,8-dihydro-2'-deoxyguanosine: implication in the 201 design of selective aptamer sensors for 8-oxo-7,8-dihydroguanine. *Anal Chem* 2013;**85**:201–7. 203
- Kroner C, Thunemann M, Vollmer S, Kinzer M, Feil R, Richert C. 204 Endless: A purine-binding RNA motif that can be expressed in cells. 205 *Angew Chem Int Ed* 2014;**53**:9198–202. 206
- Huang H, Tlatelpa PC. Tuning the selectivity of triplex DNA receptors. 207 *Chem Commun* 2015;**51**:5337–9. 208
- Zhuang Z, Pan R, Zhang Q, Huang H. Molecular recognition of 209 pyrimidine nucleobases by triplex DNA receptors. *Bioorg Med Chem Lett* 2015;**25**:1520–4. 211
- Olinski R, Rozalski R, Gackowski D, Foksinski M, Siomek A, Cooke MS. 212 Urinary measurement of 8-Oxo-dG, 8-OxoGua, and 5HMUra: A noninvasive 213 assessment of oxidative damage to DNA. *Antioxid Redox Signal* 2006;**8**:1011–9. 214
- Chiou CC, Chang PY, Chan EC, Wu TL, Tsao KC, Wu JT. Urinary 8- 215 hydroxydeoxyguanosine and its analogs as DNA marker of oxidative 216 stress: Development of an ELISA and measurement in both bladder and 217 prostate cancers. *Clin Chim Acta* 2003;**334**:87–94. 218
- Wu LL, Chiou CC, Chang PY, Wu JT. Urinary 8-OHdG: A marker of 219 oxidative stress to DNA and a risk factor for cancer, atherosclerosis and 220 diabetics. *Clin Chim Acta* 2004;**339**:1–9. 221
- Ravanat JL, Guicherd P, Tuce Z, Cadet J. Simultaneous determination of five 222 oxidative DNA lesions in human urine. *Chem Res Toxicol* 1999;**12**:802–8. 223
- Weimann A, Belling D, Poulsen HE. Quantification of 8-oxo-guanine 224 and guanine as the nucleobase, nucleoside and deoxynucleoside forms in 225 human urine by high-performance liquid chromatography–electrospray 226 tandem mass spectrometry. *Nucleic Acids Res* 2002;**30**:e7. 227
- Song MF, Li YS, Ootsuyama Y, Kasai H, Kawai K, Ohta M, et al. 228 Urea, the most abundant component in urine, cross-reacts with a 229 commercial 8-OH-dG ELISA kit and contributes to overestimation of 230 urinary 8-OH-dG. *Free Radic Biol Med* 2009;**47**:41–6. 231
- Tan LH, Xing H, Lu Y. DNA as a powerful tool for morphology control, 232 spatial positioning, and dynamic assembly of nanoparticles. *Acc Chem Res* 2014;**47**:1881–90. 234

- 235 13. Jones MR, Seeman NC, Mirkin CA. Nanomaterials. Programmable
236 materials and the nature of the DNA bond. *Science* 2015;**347**:1260901.
237 14. Xu X, Rosi NL, Wang YH, Huo FW, Mirkin CA. Asymmetric
238 functionalization of gold nanoparticles with oligonucleotides. *J Am*
239 *Chem Soc* 2006;**128**:9286-7.
240 15. Xu X, Georganopoulou DG, Hill HD, Mirkin CA. Homogeneous
241 detection of nucleic acids based upon the light scattering properties of
242 silver-coated nanoparticle probes. *Anal Chem* 2007;**79**:6650-4.
243 16. Xu X, Han MS, Mirkin CA. A gold-nanoparticle-based real-time
244 colorimetric screening method for endonuclease activity and inhibition.
245 *Angew Chem Int Ed Engl* 2007;**46**:3468-70.
246 17. Wu P, Hwang K, Lan T, Lu Y. A DNAzyme-gold nanoparticle probe for
247 uranyl ion in living cells. *J Am Chem Soc* 2013;**135**:5254-7.
248 18. Jensen SA, Day ES, Ko CH, Hurley LA, Luciano JP, Kouri FM, et al.
249 Spherical nucleic acid nanoparticle conjugates as an RNAi-based therapy
250 for glioblastoma. *Sci Transl Med* 2013;**5**:209ra152.
19. Xu X, Daniel WL, Wei W, Mirkin CA. Colorimetric Cu(2+) detection
251 using DNA-modified gold-nanoparticle aggregates as probes and click
252 chemistry. *Small* 2010;**6**:623-6. 253
20. Zhang XQ, Xu X, Lam R, Giljohann D, Ho D, Mirkin CA. Strategy for
254 increasing drug solubility and efficacy through covalent attachment to
255 polyvalent DNA-nanoparticle conjugates. *ACS Nano* 2011;**5**:6962-70. 256
21. Rosi NL, Mirkin CA. Nanostructures in biodiagnostics. *Chem Rev*
257 2005;**105**:1547-62. 258
22. Marca GL, Casetta B, Malvagia S, Pasquini E, Innocenti M, Donati MA,
259 et al. Implementing tandem mass spectrometry as a routine tool for
260 characterizing the complete purine and pyrimidine metabolic profile in
261 urine samples. *J Mass Spectrom* 2006;**41**:1442-52. 262
23. Cooke MS, Olinski R, Loft S. Members of the European Standards
263 Committee on Urinary (DNA) Lesion Analysis (ESCUA). Measurement
264 and meaning of oxidatively modified DNA lesions in urine. *Cancer*
265 *Epidemiol Biomarkers Prev* 2008;**17**:3-14. 266
267



ELSEVIER

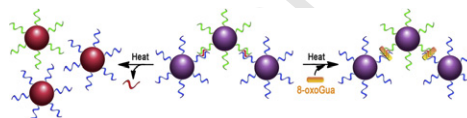
Nanomedicine: Nanotechnology, Biology, and Medicine
xx (2016) xxx–xxxnanomedicine
Nanotechnology, Biology, and Medicine

nanomedjournal.com

Graphical Abstract

Highly specific colorimetric detection of DNA oxidation biomarker using gold nanoparticle/triplex DNA conjugates*Nanomedicine: Nanotechnology, Biology, and Medicine xxx (2016) xxx–xxx*Xun Gao, PhD^a, Yung-Hao Tsou, PhD^b, Marina Garis^b,
Haidong Huang, PhD^{a,*}, Xiaoyang Xu, PhD^{b,*}^aDepartment of Chemistry and Environmental Science, New Jersey Institute of Technology, Newark, NJ, USA^bDepartment of Chemical, Biological, and Pharmaceutical Engineering, New Jersey Institute of Technology, Newark, NJ, USA

The gold nanoparticle/triplex DNA conjugates contained a pre-organized cavity that can bind 8-oxoGua with strong affinity and excellent selectivity over other nucleobases. Nanoparticle assemblies interconnected with DNA triple helices bound with 8-oxoGua show much sharper and significantly higher melting temperatures than the analogous free DNA triplex. By simply incubating our sensor with a urine sample, 8-oxoGua can be detected colorimetrically at submicromolar concentrations with a UV–vis spectrometer or even by naked eyes.



UNCORRECTED PRC